ISSN 2070-0504, Catalysis in Industry, 2019, Vol. 11, No. 2, pp. 87–94. © Pleiades Publishing, Ltd., 2019.
Russian Text © The Author(s), 2018, published in Kataliz v Promyshlennosti.

GENERAL PROBLEMS OF CATALYSIS

Key Stages in the Formation of $AlPO_4$-11 via the Crystallization of a Boehmite-Based Aluminophosphate Gel

M. R. Agliullin[a, b, *], Z. R. Khairullina[b], A. V. Faizullin[a], A. I. Petrov[b], A. A. Badretdinova[b], V. P. Talzi[c], and B. I. Kutepov[a, b]

[a] *Institute of Petrochemistry and Catalysis, Ufa Federal Research Center, Russian Academy of Sciences, Ufa, Republic of Bashkortostan, 450075 Russia*

[b] *Ufa State Petroleum Technological University, Ufa, Republic of Bashkortostan, 450000 Russia*

[c] *Institute of Problems of Hydrocarbon Processing, Siberian Branch, Russian Academy of Sciences, Omsk, 644040 Russia*

**e-mail: maratradikovich@mail.ru*

Received April 20, 2018; revised June 19, 2018; accepted July 6, 2018

Abstract—The staged crystallization of aluminophosphate $AlPO_4$-11 from a commercially available aluminum source based on boehmite is studied for the first time by means of X-ray diffraction, ^{27}Al and ^{31}P magic-angle spinning nuclear magnetic resonance, low-temperature nitrogen adsorption–desorption, and scanning election microscopy. It is shown that the synthesis of $AlPO_4$-11 proceeds via the formation of an intermediate phase based on crystalline aluminophosphate with a layered structure. It is found that $AlPO_4$-11 with a high degree of crystallinity and phase purity forms in 6–24 h at 200°C. Lengthening the time of crystallization at 200°C to more than 48 h results in the transformation of $AlPO_4$-11 into nonporous cristobalite. The results can be used to develop means for directional control of the phase purity and degree of crystallinity of commercially important silicoaluminophosphate molecular sieves SAPO-11 with desired properties. These can be used as a base for the synthesis of promising domestic catalysts for the commercial hydroisomerization of higher *n*-paraffins.

Keywords: zeolites, aluminophosphate $AlPO_4$-11, crystallization, boehmite, *n*-paraffin hydroisomerization

DOI: 10.1134/S2070050419020028

INTRODUCTION

Zeolites and zeolite-like materials are commonly used as heterogeneous catalysts, adsorbents, and ion-exchange materials, due to the presence of acid sites, a developed microporous structure, and a molecular sieve effect in them [1–6].

Due to the presence of a one-dimensional channel system of pores and medium-strength acid sites in aluminophosphate ($AlPO_4$-11) and silicoaluminophosphate molecular sieves (SAPO-11), these materials are of considerable interest as promising catalyst systems for the hydroisomerization of higher *n*-paraffins. However, issues over the crystallization mechanism of these materials remain poorly studied.

In 1982, Wilson et al. [8, 9] reported the synthesis of a new class of zeolite-like materials based on aluminophosphates $AlPO_4$-*n* (*n* indicates the type of structure). The $AlPO_4$-*n* structure is composed of strictly alternating AlO_4 and PO_4 tetrahedra linked through their oxygen atoms. Aluminophosphates with one-dimensional, two-dimensional, and three-dimensional channel structures have been synthesized: $AlPO_4$-11, $AlPO_4$-40, and $AlPO_4$-18, respectively [10]. The sizes of the entrance windows in aluminophosphates can vary in the range of 3–12 Å. These materials are of considerable interest as matrices for the development of single-site catalysts for liquid-phase oxidation, since they are capable of isomorphously incorporating variable-valence metal atoms into their crystal lattices [11–16]. At the same time, introducing atoms of such elements as Si or Mg into the aluminophosphate lattice produces acid sites that are weaker than those in aluminosilicates [17–20].

Among the wide variety of aluminophosphates, of particular interest is aluminophosphate $AlPO_4$-11 with a one-dimensional system of 10-membered elliptic channels 0.40 × 0.65 nm in size [10]; it has been used as a base for synthesizing silicoaluminophosphate SAPO-11 and developing promising catalyst systems for the hydroisomerization of higher *n*-paraffins [21], the methylation of aromatic hydrocarbons [22], the isomerization of butylene to isobutylene [23], and the isomerization of cyclohexanone oxime to caprolactam [24].

Researchers have given much attention to studying the crystallization mechanism of $AlPO_4$-11; an understanding of this mechanism is required for developing

ways of controlling the phase purity and degrees of crystallinity and dispersion of the synthesized aluminophosphates, and thus silicoaluminophosphate molecular sieves with desired properties. Using *ex situ* X-ray diffraction (XRD) and ^{27}Al and ^{31}P magic-angle spinning nuclear magnetic resonance (MAS NMR), the authors of [25, 26] studied the crystallization of $AlPO_4$-11 from aluminophosphate gels of different concentrations, prepared using pseudoboehmite (AlO((OH)) as an aluminum source. It was shown that in the dilute gels, $AlPO_4$-5 forms at the initial stage of crystallization; afterward, it transforms into $AlPO_4$-11. The intermediate formation of $AlPO_4$-5 is not observed in concentrated gels.

The crystallization of $AlPO_4$-11 from aluminophosphate gels prepared using phosphoric acid and $Al(OH)_3$ was studied by the authors of [27] by means of two-dimensional ^{27}Al and ^{31}P MAS NMR and Fourier transform Raman spectroscopy. It was found that at room temperature, amorphous aluminophosphate can form even at the initial stage of gel preparation. The formation of an intermediate semicrystalline phase was also observed, but the structure of this phase was not determined.

The crystallization of $AlPO_4$-11 from dry gels, also prepared using phosphoric acid and $Al(OH)_3$, was studied via *ex situ* XRD and ^{27}Al and ^{31}P MAS NMR in [28]. It was shown that a semicrystalline phase containing fragments of 10-membered rings forms at the initial stages of crystallization. The cited authors assumed that the local structure of this phase was fairly close to that of $AlPO_4$-11, and the former was rapidly transformed into the latter. However, the structure of the intermediate phases was not fully determined either.

Despite the considerable number of works on the synthesis of $AlPO_4$-11 [25–36], the mechanism of this aluminophosphate's crystallization thus remains poorly understood. The aim of this work was to study the key stages of the formation of $AlPO_4$-11 via crystallization from an aluminophosphate gel prepared using an industrial feedstock (boehmite) as an aluminum source.

EXPERIMENTAL

Aluminophosphate Synthesis Procedure

All aluminophosphate samples were prepared via hydrothermal synthesis from a reaction gel of the following composition: $1.0Al_2O_3 \cdot 1.0P_2O_5 \cdot 1.0$ di-*n*-propylamine (DPA) $\cdot$ $50H_2O$. The sources of phosphorus and aluminum were phosphoric acid (85% H_3PO_4, Reakhim, Russia) and boehmite (81% Al_2O_3, OOO Ishimbay Specialized Chemical Plant of Catalysts, Russia), respectively; DPA (99%, Acros Organics) was used as a template. The aluminophosphate gel was prepared as follows: 50.0 g of phosphoric acid was diluted with 178.0 g of distilled water; 27.5 g of boehmite was added to the resulting solution; the mixture was vigorously stirred for 1 h. Next, 22 g of DPA was added to the resulting gel, and the mixture was held in a thermostat at 90°C for 24 h. It was shown in [37] that the original gel must be held at 90°C to ensure the subsequent selective crystallization of $AlPO_4$-11. The prepared gel is designated $AlPO_4$(90°C). The crystallization of aluminophosphates was conducted at 200°C in a stainless steel autoclave (SEN, $V = 1000$ mL) with a special fluoroplastic coating and a sampling system. The products of crystallization were sampled after 1, 3, 6, 12, 24, 48, and 72 h. The aluminophosphate samples synthesized from the $AlPO_4$(90°C) gel were designated as $AlPO_4$-11-*n*, where *n* is the period of crystallization.

Investigation Procedure

X-ray diffraction analysis of the samples was performed on a Rigaku Ultima IV diffractometer using monochromatized CuK_α radiation. Scanning was done in a 2θ angular range of 3°–80° in increments of 0.5 deg/min; acquisition time was 2 s per point. The XRD patterns were processed using the Rigaku PDXL software and the PDF2 database.

The coordination environment of the aluminum and phosphorus atoms was determined from ^{27}Al and ^{31}P MAS NMR spectra. The spectra were recorded on a Bruker Avance-400 NMR spectrometer under conditions of a single-pulse experiment, while spinning the sample at the magic angle (≈7 KHz) in zirconia rotors (Ø4 mm). The Larmor frequency was 104 (^{27}Al) and 162 MHz (^{31}P); the π/2 pulse length was 2 (^{31}P) and 2.5 μs (^{27}Al).

Micropore volume was determined from the heptane vapors in a desiccator, as described in [38]. Specific surface area and total pore volume were measured via low-temperature nitrogen adsorption–desorption on an ASAP 2020 surface area and porosimetry system. Calculations of the specific surface area using the Brunauer–Emmett–Teller (BET) approach [39] were made at a relative partial pressure of $P/P_0 = 0.2$.

The morphology of the aluminophosphates was studied via scanning electron microscopy (SEM) on a JEOL JSM-6490LV electron microscope. Images were recorded in the secondary electron imaging mode at an accelerating voltage of 20 kV and a working distance of 10 mm. Before recording, the samples were placed on the surface of an aluminum table with a diameter of 25 mm and fixed there using a conductive adhesive tape.

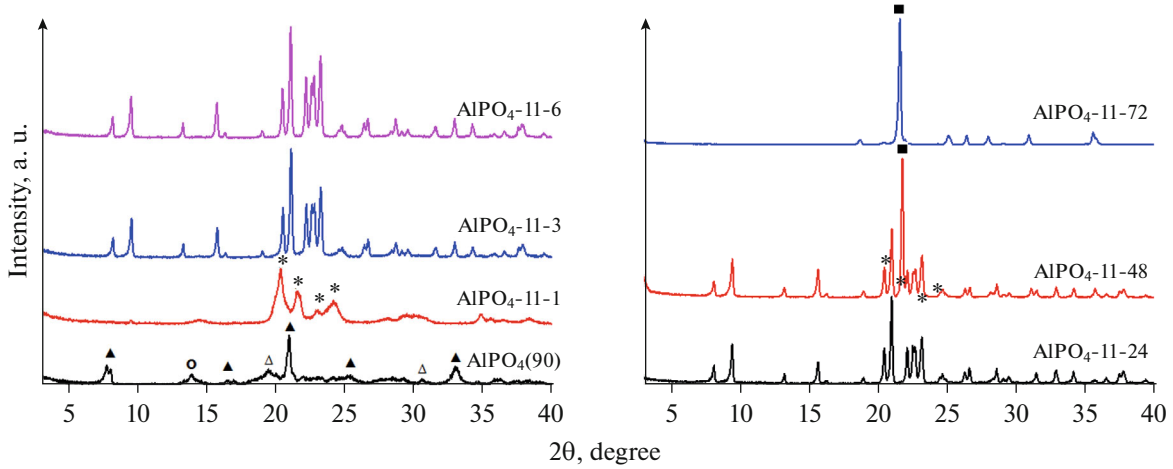

Fig. 1. X-ray diffraction analysis data for aluminophosphate samples synthesized with different periods of crystallization: (▲) DPA phosphate, (**O**) boehmite, (△) variscite, (*) intermediate crystalline aluminophosphate, and (■) cristabolite.

RESULTS AND DISCUSSION

Dependence of the Phase Composition of the Products of Crystallization on the Period of Synthesis

Figure 1 shows XRD patterns of the original gel and the products of crystallization formed at varying times of synthesis. Different phases were observed in the original $AlPO_4$(90°C) gel sample: DPA phosphate (30 vol %), undissolved boehmite (10 vol %), amorphous aluminophosphate (60 vol %), and variscite (10 vol %). It is evident that the subsequent crystallization of the gel for 1 h at 200°C (sample $AlPO_4$-11-1) results in the formation of an intermediate $AlPO_4$ crystalline aluminophosphate phase (PDF 00-201-0795). According to XRD, this material has a rhombic syngony with an average coherent scattering region (CSR) of ≈10 nm. After 3 h of crystallization (sample $AlPO_4$-11-3), the main phase was $AlPO_4$-11, and a small amount of unreacted boehmite was observed. It should be noted that 24 h of crystallization led to complete dissolution of the unreacted boehmite and the formation of $AlPO_4$-11 with a degree of crystallinity of ≈100% (sample $AlPO_4$-11-24). Lengthening the period of crystallization past 24 h (sample $AlPO_4$-11-48) produced a new phase of crystalline aluminophosphate with a cristobalite structure. After 72 h (sample $AlPO_4$-11-72), complete recrystallization of the $AlPO_4$-11 into cristobalite was observed.

More detailed information on the chemical nature of aluminophosphates formed during the initial period of crystallization could be obtained via ^{27}Al and ^{31}P MAS NMR spectroscopy. Figure 2 shows ^{27}Al and ^{31}P MAS NMR spectra for the original gel and the products obtained at different periods of synthesis.

It is evident that the ^{27}Al MAS NMR spectra of the original gel (Fig. 2a) exhibit characteristic signals at 48, 12, and −9 ppm. The authors of [33–36] attributed the signal at 48 ppm to tetrahedrally coordinated aluminum atoms that were part of the alumophosphate sol particles. The signal at 12 ppm is characteristic of octahedrally coordinated aluminum atoms contained in undissolved boehmite. The signal at −9 ppm corresponds to octahedrally coordinated aluminum atoms that were part of nonporous aluminophosphates. Crystallizing the $AlPO_4$(90°C) gel for 1 h considerably weakened the signal at 12 ppm and amplified the signal at −9 ppm. The results are attributed to the interaction between previously unreacted boehmite and phosphoric acid, and the formation of an intermediate crystalline aluminophosphate. This assumption is in good agreement with the XRD data (see Fig. 1). Three hours of crystallization substantially reduced the fraction of the signal at −9 ppm and produces a new signal at 42 ppm, which is characteristic of tetrahedral aluminum in the crystal lattice of $AlPO_4$-11. Twenty-four hours of crystallization resulted in complete disappearance of the signal at −9 ppm and amplification of the signal at 42 ppm.

According to ^{31}P MAS NMR (Fig. 2b), the spectra of the original gels exhibit signals at 38, 27, 5, −8, and −15 ppm. The authors of [40, 41] attributed the signal at 5 ppm to phosphates of nitrogen-containing organic compounds. This signal is apparently associated with DPA phosphate, the presence of which was confirmed by XRD data for the original gel (Fig. 1, sample $AlPO_4$-11-1). The signals at −8 and −15 ppm were attributed to tetrahedrally coordinated phosphorus atoms in aluminophosphates with different degrees of replacing –OH groups with aluminum atoms [33–36]. The signals at 27 and 38 ppm were attributed to tetrahedrally coordinated P atoms in the crystalline structure of the zeolite.

The spectral data show that the original $AlPO_4$(90°C) gel exhibited signals at 5 and 8 ppm and an intense signal at 15 ppm. These signals suggest that

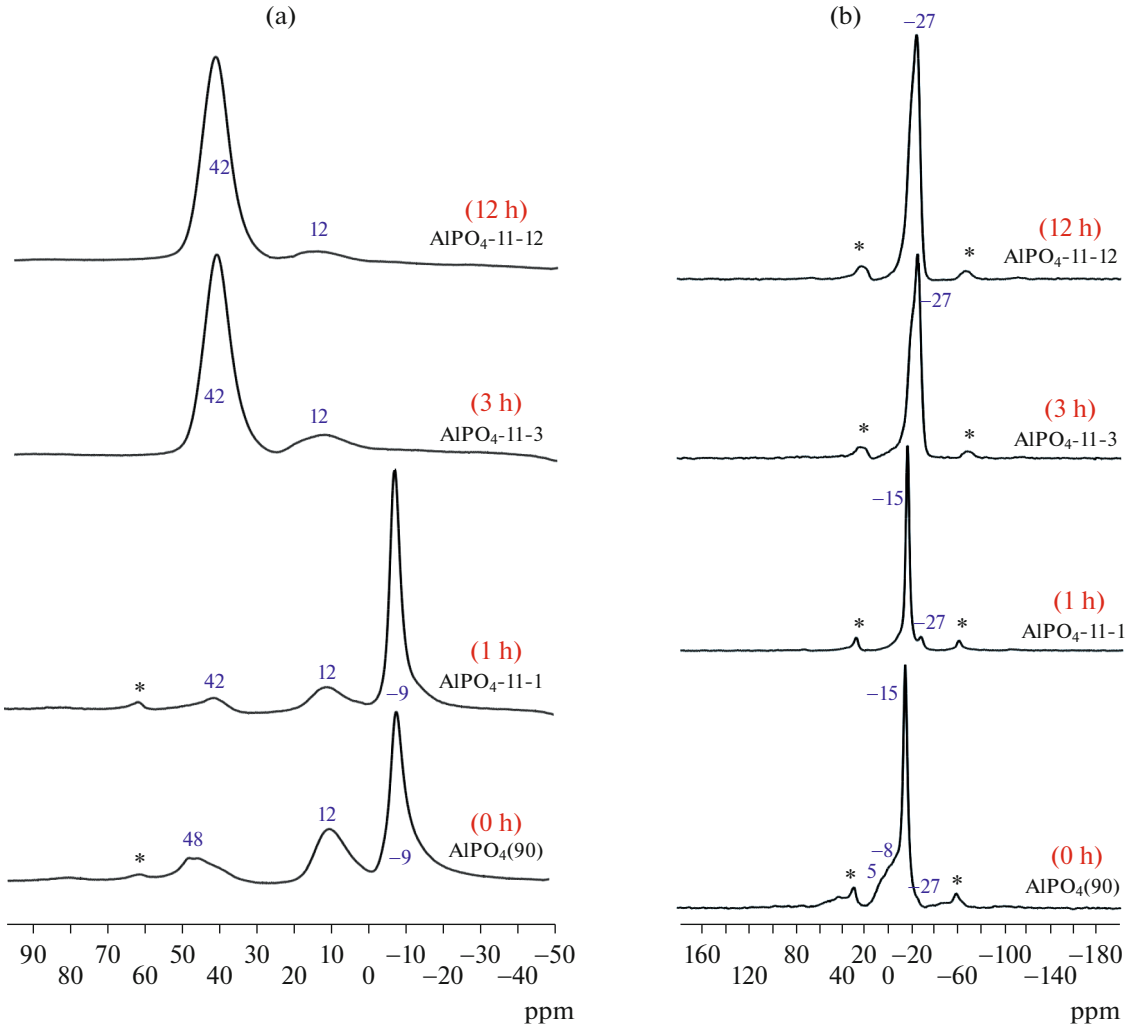

Fig. 2. (a) ^{27}Al and (b) ^{31}P MAS NMR data for the aluminophosphate samples synthesized with different periods of crystallization.

most of the P atoms were present in the form of aluminophosphates with different fractions of P–O–Al bonds. This is in good agreement with the XRD and ^{27}Al MAS NMR data. After 1 h of crystallization, the spectrum exhibited the main signal at −15 ppm. This indicates the formation of an intermediate crystalline aluminophosphate phase (Fig. 1, sample $AlPO_4$-11-1). After 3 h of crystallization, an intense signal at 27 ppm, associated with the presence of tetrahedrally coordinated P atoms in the lattice of $AlPO_4$-11, appeared in the spectrum. Lengthening the period of crystallization to 24 h produced a single signal at 27 ppm (spectrum not shown), testifying to the high degree of crystallinity of the synthesized material.

Dependence of the Pore Structure of Crystallization Products on the Period of Synthesis

Table 1 shows characteristics of the pore structure of the aluminophosphate samples prepared at varying periods of crystallization. It is evident the intermediate crystalline aluminophosphate that formed after 1 h (sample $AlPO_4$-11-1) was a porous material with a total pore volume of $V_\Sigma = 0.45$ cm^3/g and a BET specific surface area of 80 m^2/g. Figure 3 shows the adsorption–desorption isotherm and the pore size distribution for this sample. It is evident that this material was a meso/macroporous system with a broad pore size distribution in the range of 2–300 nm. A reduction in the total pore volume (to 0.15 cm^3/g) and in the specific surface area (to 132 m^2/g) was observed after 3 h of crystallization (sample $AlPO_4$-11-3). Lengthening the period of crystallization to 24 h (sample $AlPO_4$-11-24) produces $AlPO_4$-11 with a high degree of crystallinity, a pore volume of $V_{C_7H_{16}} = 0.14$ cm^3/g with respect to heptane, a total pore volume of $V_\Sigma = 0.16$ cm^3/g, and a specific surface area of $S_{BET} \approx 110$ m^2/g. These results are in good agreement with the published data for aluminophosphate $AlPO_4$-11 [25–32]. Lengthen-

Table 1. Characteristics of the pore structure of crystalline aluminophosphates*

Sample	$V_{C_7H_{16}}$, cm^3/g	V_Σ, cm^3/g	S_{BET}, m^2/g	Particle size (according to SEM), μm
$AlPO_4$-11-1	0.30	0.45	80	3–5
$AlPO_4$-11-3	0.17	0.15	132	1–2
$AlPO_4$-11-12	0.14	0.16	112	1–2
$AlPO_4$-11-24	0.14	0.16	110	1–2
$AlPO_4$-11-48	0.03	0.09	60	50
$AlPO_4$-11-72	0.00	0.02	10	50

*V_Σ is the total micropore volume, $V_{C_7H_{16}}$ is the micropore volume with respect to heptane vapors, and S_{BET} is the specific surface area determined via BET.

ing the period of crystallization past 48 h (sample $AlPO_4$-11-48) further reduces the total pore volume to $V_\Sigma = 0.09$ cm^3/g and the specific surface area to $S_{BET} \approx 60$ m^2/g.

The above data suggest that the intermediate crystalline aluminophosphate ($AlPO_4$-11-1 sample) formed in the initial period of crystallization is characterized by a developed meso/macroporous structure. The subsequent transformation of this aluminophosphate into $AlPO_4$-11 lowers the specific surface area and the volume of micro- and mesopores. The recrystallization of $AlPO_4$-11 into cristobalite further reduces in the pore volume and the specific surface area.

Dependence of the Morphology of Crystallization Products on the Period of Synthesis

Figure 4 shows SEM images of aluminophosphate samples prepared at varying periods of crystallization. It is evident that the $AlPO_4$-11-1 sample consists of thin layered crystals 10–20 nm thick, which is in good agreement with the CSR value of around 10 nm. According to SEM, the pore size of this aluminophosphate is 100–300 nm. It should be noted that in the 2θ range of 3°–7°, the XRD pattern of the sample ($AlPO_4$-11-1) exhibits none of the signals characteristic of layered materials, due to its large interplanar distances. According to XRD and ^{27}Al and ^{31}P MAS NMR, this sample is a crystalline aluminophosphate. According to XRD and ^{27}Al and ^{31}P MAS NMR, after 3 h of crystallization ($AlPO_4$-11-3 sample), the dominant phase is $AlPO_4$-11 (90%) with the crystal morphology in the form of thin plates 1–2 μm in size. Upon reaching the maximum degree of crystallinity after 6 h (sample $AlPO_4$-11-6), the crystal morphology remained unchanged in the form of thin rectangular plates.

As noted above, $AlPO_4$-11 was transformed into cristobalite after 48 h of crystallization. The image of the $AlPO_4$-11-48 sample shows large (30–40 μm) crystals in the form of truncated octahedra; in addition, a small number of the remaining parts of $AlPO_4$-11 crystals is observed.

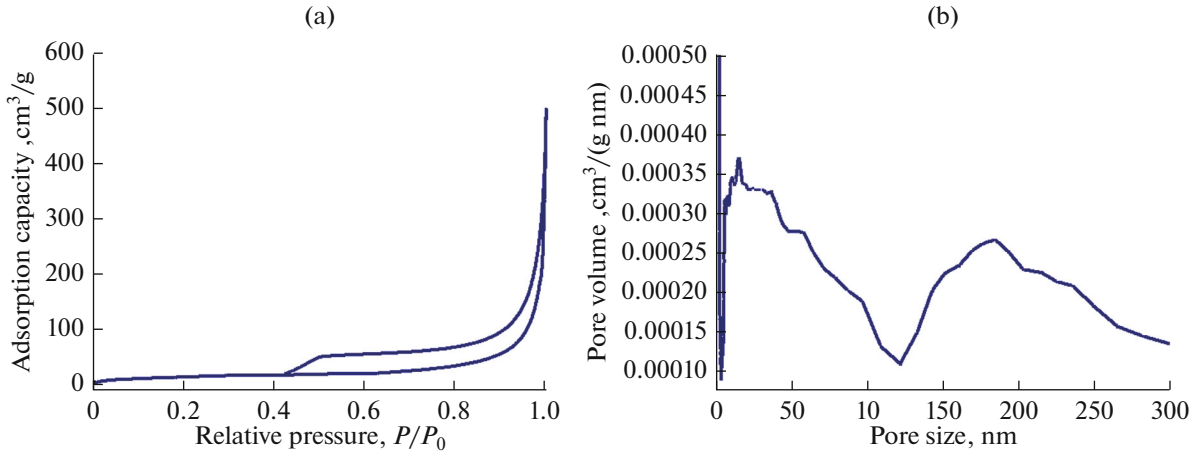

Fig. 3. (a) Nitrogen adsorption–desorption isotherm and (b) pore size distribution for the intermediate crystalline aluminophosphate sample ($AlPO_4$-11-1).

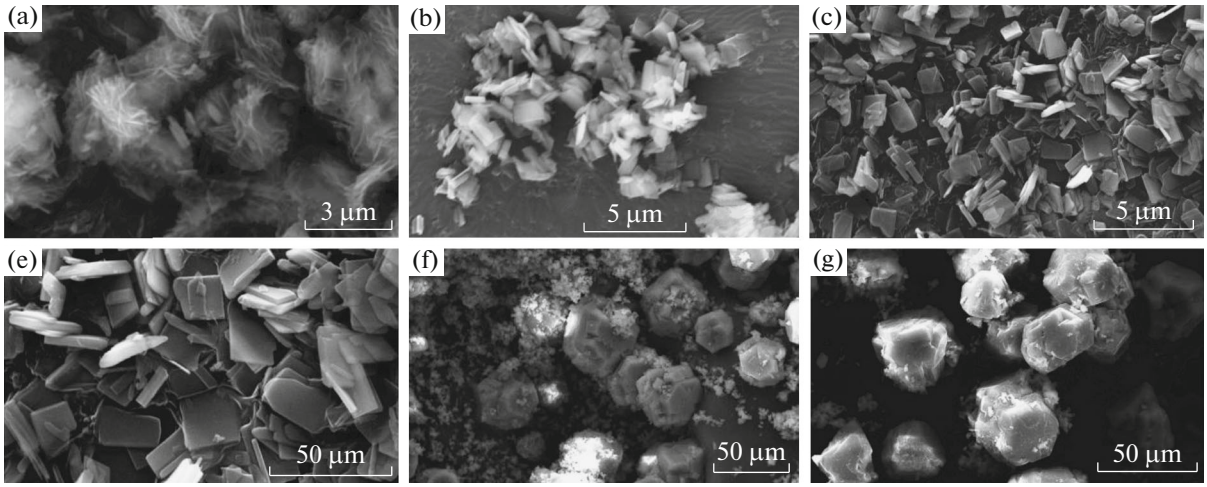

Fig. 4. SEM photos of aluminophosphate samples synthesized with different periods of crystallization: (a) $AlPO_4$-11-1, (b) $AlPO_4$-11-3, (c) $AlPO_4$-11-6, (d) $AlPO_4$-24, (e) $AlPO_4$-11-48, and (f) $AlPO_4$-11-72.

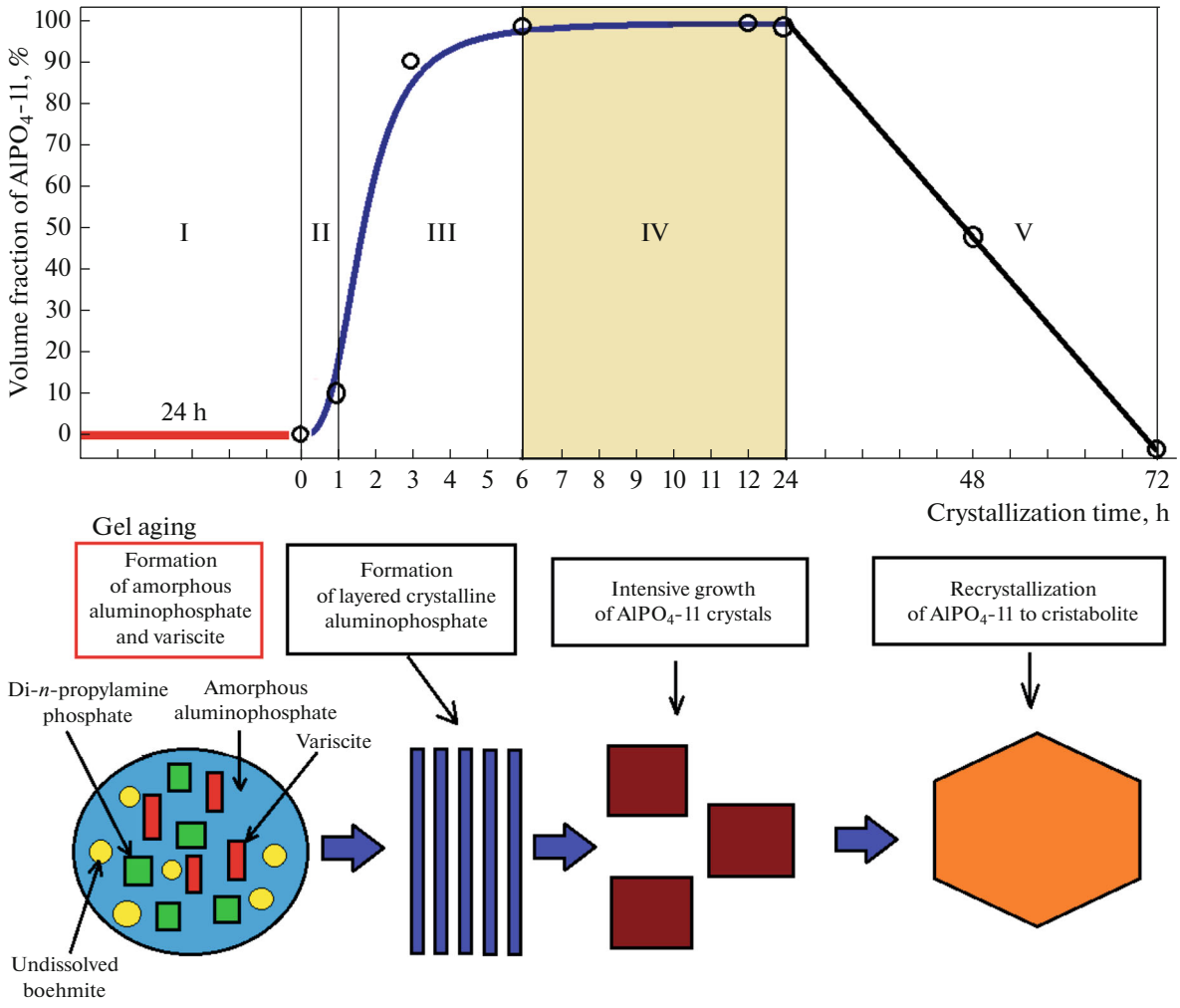

Fig. 5. Staged synthesis of $AlPO_4$-11 from aluminophosphate gel prepared using boehmite and phosphoric acid.

According to XRD, 72 h of crystallization resulted in the complete recrystallization of $AlPO_4$-11 into cristobalite.

Crystallization of $AlPO_4$-11 from an Aluminophosphate Gel Using Boehmite

The obtained results revealed the stages of formation of $AlPO_4$-11 from a boehmite-based aluminophosphate gel (Fig. 5). At the first stage (stage I, 90°C, 24 h), DPA phosphate reacted with undissolved boehmite to form an amorphous aluminophosphate gel and variscite; this ensured the subsequent selective crystallization of $AlPO_4$-11. At the second stage (stage II), the aluminophosphate gel was transformed into a crystalline aluminophosphate with a layered structure. The duration of this stage at 200°C was around 1 h; in the literature [1], it is commonly referred to as the induction period, the stage at which nuclei form. At the third stage (stage III), $AlPO_4$-11 crystals grew intensely for 3–6 h. The layered aluminophosphate simultaneously transformed almost completely into $AlPO_4$-11, while unreacted boehmite and the amorphous phase dissolved. The $AlPO_4$-11 content was 90% after 6 h of crystallization. Upon lengthening the period of crystallization from 6 to 24 h (stage IV), the $AlPO_4$-11 content was ≈100%; in the literature, this stage is referred to as aging of the system. Lengthening the period of synthesis further to 72 h (stage V) resulted in the recrystallization of $AlPO_4$-11 into cristobalite (see Fig. 4).

CONCLUSIONS

The kinetics of the crystallization (200°C) of an aluminophosphate gel prepared from phosphoric acid and boehmite into commercially important $AlPO_4$-11 with a high degree of crystallinity and phase purity was studied via XRD, ^{27}Al and ^{31}P MAS NMR, low-temperature nitrogen adsorption–desorption, and SEM.

It was found that the formation of $AlPO_4$-11 proceeds through the stages of

- holding the gel at 90°C (24 h) to ensure the subsequent selective crystallization of $AlPO_4$-11;
- an induction period around 1 h long to ensure the formation of an intermediate phase based on crystalline aluminophosphate with a layered structure;
- intense growth of $AlPO_4$-11 crystals for 3–6 h; and
- recrystallization of $AlPO_4$-11 into cristobalite.

It was found that AlPO4-11 with a high degree of crystallinity and phase purity forms in 6–24 h at 200°C. Upon lengthening the period of crystallization at 200°C to more than 48 h, we observed the transformation of $AlPO_4$-11 into nonporous cristobalite.

The results will be used to develop means for the directional control of the phase purity and degree of crystallinity of commercially important silicoaluminophosphate molecular sieves with desired properties.

ACKNOWLEDGMENTS

The synthesized materials were analyzed using equipment at the Agidel Shared Resource Center of the Institute of Petrochemistry and Catalysis of the Russian Academy of Sciences.

FUNDING

This work was supported by the Russian Science Foundation, project no. 18-73-00007.

REFERENCES

1. Cejka, J., Corma, A., and Zones, S., *Zeolites and Catalysis: Synthesis, Reactions and Applications,* Weinheim: Wiley-VCH, 2010.
2. Degnan Jr, T. F., *Stud. Surf. Sci. Catal.,* 2007, vol. 170, pp. 54–65.
3. Moliner, M., Martínez, C., and Corma, A., *Angew. Chem., Int. Ed.,* 2015, vol. 54, no. 12, pp. 3560–3579.
4. Chal, R., Gérardin, C., Bulut, M., and van Donk, S., *ChemCatChem,* 2011, vol. 3, no. 1, pp. 67–81.
5. *Zeolite Characterization and Catalysis: A Tutorial,* Chester, A.W. and Derouane, E.G., Eds., New York: Springer 2009.
6. Wright, P.A., *Microporous Framework Solids,* Cambridge: Royal Society of Chemistry, 2008.
7. Xu, R., Pang, W., Yu, J., Huo, Q., and Chen, J., *Chemistry of Zeolites and Related Porous Materials: Synthesis and Structure,* Singapore: Wiley, 2007.
8. Wilson, S.T., Lok, B.M., Messina, C.A., Cannan, T.R., and Flanigen, E.M., *J. Am. Chem. Soc.,* 1982, vol. 104, no. 4, pp. 1146–1147.
9. US Patent 4310440, 1982.
10. Baerlocher, C., McCusker, L.B., and Olson, D.H., *Atlas of Zeolite Framework Types,* New York: Elsevier, 2007.
11. Thomas, J.M., Raja, R., Sankar, G., and Bell, R.G., *Nature,* 1999, vol. 398, no. 6724, pp. 227–230.
12. Inui, T., Matsuda, H., Okaniwa, H., and Miyamoto, A., *Appl. Catal.,* 1990, vol. 58, no. 1, pp. 155–163.
13. Thomas, J.M., Xu, Y., Catlow, C.R.A., and Couves, J.W., *Chem. Mater.,* 1991, vol. 3, no. 4, pp. 667–672.
14. Liu, Y., Liu, C., Liu, C., Tian, Z., and Lin, L., *Energy Fuels,* 2004, vol. 18, no. 5, pp. 1266–1271.
15. Rastelli Jr, H., Lok, B.M., Duisman, J.A., Earls, D.E., and Mullhaupt, J.T., *Can. J. Chem. Eng.,* 1982, vol. 60, no. 1, pp. 44–49.
16. Thomas, J.M., Raja, R., Sankar, G., and Bell, R.G., *Acc. Chem. Res.,* 2001, vol. 34, no. 3, pp. 191–200.
17. Pastore, H.O., Coluccia, S., and Marchese, L., *Annu. Rev. Mater. Res.,* 2005, vol. 35, pp. 351–395.
18. Liu, Y., Yan, A.Z., and Xu, Q.H., *Appl. Catal.,* 1990, vol. 67, pp. 169–177.
19. Borade, R.B. and Clearfield, A., *J. Mol. Catal.,* 1994, vol. 88, no. 2, pp. 249–266.

20. Tao, S., Li, X., Gong, H., Jiang, Q., Yu, W., Ma., H., Xu, R., Tian, Z., *Microporous Mesoporous Mater.,* 2018, vol. 262, pp. 182–190.
21. Walendziewski, J. and Pniak, B., *Appl. Catal., A,* 2003, vol. 250, no. 1, pp. 39–47.
22. Zhu, Z., Chen, Q., Xie, Z., and Yang, W., *Microporous Mesoporous Mater.,* 2006, vol. 88, nos. 1–3, pp. 16–21.
23. Yang, S.-M., Lin, J.-Y., Guo, D.-H., and Liaw, S.-G., *Appl. Catal., A,* 1999, vol. 181, no. 1, pp. 113–122.
24. Singh, P.S., Bandyopadhyay, R., Hegde, S.G., and Rao, B.S., *Appl. Catal., A,* 1996, vol. 136, no. 2, pp. 249–263.
25. Cheng, T., Xu, J., Li, X., Li, Y., Zhang, B., Yan, W., Yu, J., Sun, H., Deng, F., and Xu, R., *Microporous Mesoporous Mater.,* 2012, vol. 152, pp. 190–207.
26. Zhang, B., Xu, J., Fan, F., Guo, Q., Tong, X., Yan, W., Yu, J., Deng, F., Li, C., and Xu, R., *Microporous Mesoporous Mater.,* 2012, vol. 147, no. 1, pp. 212–221.
27. Huang, Y., Richer, R., and Kirby, C.W., *J. Phys. Chem. B,* 2003, vol. 107, no. 6, pp. 1326–1337.
28. Chen, B. and Huang, Y., *J. Phys. Chem. C,* 2007, vol. 111, no. 42, pp. 15236–15243.
29. Balakrishnan, I. and Prasad, S., *Appl. Catal.,* 1990, vol. 62, no. 1, pp. L7–L11.
30. Qisheng, H. and Xu, R., *J. Chem. Soc., Chem. Commun.,* 1990, no. 10, pp. 783–784.
31. Ojo, A.F. and McCusker, L.B., *Zeolites*, 1991, vol. 71, no. 5, pp. 460–465.
32. Zhao, X., Gao, X., Zhang, X., and Hao, Z., *Microporous Mesoporous Mater.,* 2017, vol. 242, pp. 160–165.
33. Zhao, Z., Zhang, W., Xu, R., Han, X., Tiana, Z., and Bao, X., *Dalton Trans.,* 2012, vol. 41, no. 3, pp. 990–994.
34. Tapp, N.J., Milestone, N.B., and Bibby, D.M., *Zeolites,* 1988, vol. 8, no. 3, pp. 183–188.
35. Zhu, G., Qiu, S., Gao, F., Wu, G., Wang, R., Li, B., Fang, Q., Li, Y., Gao, B., Xu, X., and Terasaki, O., *Microporous Mesoporous Mater.,* 2001, vol. 50, nos. 2–3, pp. 129–135.
36. Bandyopadhyay, M., Bandyopadhyay, R., Kubota, Y., and Sugi, Y., *Chem. Lett.,* 2000, vol. 29, no. 9, pp. 1024–1025.
37. Agliullin, M.R., Khairullina, Z.R., Faizullin, A.V., Petrov, A.I., Badretdinova, A.A., and Kutepov, B.I., Abstract of Papers, *Materialy 8 Vserossiiskoi tseolitnoi konferentsii* (Proc. Eighth All-Russian Zeolite Conference), 2018, pp. 64–65.
38. Kel'tsev, N.V., *Osnovy adsorbtsionnoi tekhniki* (Principles of Adsorption Technique), Moscow: Khimiya, 1984.
39. Gregg, S.J., Sing, K.S.W., and Salzberg, H.W., *J. Electrochem. Soc.,* 1967, vol. 114, no. 11, p. 279.
40. Tong, X., Xu, J., Li, X., Li, Y., Yan, W., Yu, J., Deng, F., Sun, H., and Xu, X., *Microporous Mesoporous Mater.,* 2013, vol. 176, pp. 112–122.
41. Tong, X., Xu, J., Xin, L., Huang, P., Lu, H., Wang, C., Yan, W., Yu, J., Deng, F., Sun, H., and Xu, R., *Microporous Mesoporous Mater.,* 2012, vo. 164, pp. 56–66.

Translated by M. Timoshinina